The 2010 IEEE/RSJ International Conference on
Intelligent Robots and Systems
October 18-22, 2010, Taipei, Taiwan

Artificial Ridged Skin for Slippage Speed Detection in Prosthetic Hand Applications

Dana D. Damian, Harold Martinez, Konstantinos Dermitzakis, Alejandro Hernandez-Arieta and Rolf Pfeifer

***Abstract*— The human hand is one of the most complex structures in the body, being involved in dexterous manipulation and fine sensing. Traditional engineering approaches have mostly attempted to match such complexity in robotics without sufficiently stressing on the underlying mechanisms that its morphology encodes. In this work, we propose an artificial skin able to encode, through its morphology, the tactile sense of a robotic hand, characteristic to slippage events. The underlying layout consists of ridges and allows slippage detection and the quantification of slippage speed. Such encoding of slippage signal becomes suitable for relaying tactile feedback to users in prosthetic applications. This approach emphasizes the importance of exploiting morphology and mechanics in structures for the design of prosthetic interfaces.**

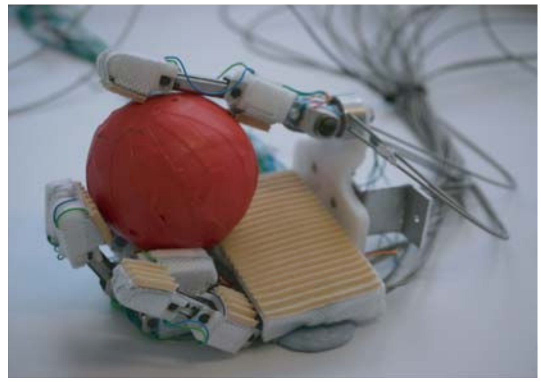

Fig. 1. Robotic hand equipped with artificial ridged skin.

I. INTRODUCTION

Haptic technology has gained interest in robotics as the means for enabling a major sense through which robots can perceive the environment and interact with it. In prosthetic applications, restoring the feedback loss is crucial for the normal functions of the human, in regards to the body awareness and its control or environment perception [1]. Slippage sensing is a prerequisite for stable grasp and fine object manipulation [2]. A wide range of interesting tactile sensors have been developed for slippage detection which use a variation of transduction principles. Cotton et al. [3] developed a thick-film piezoelectric sensor for slippage detection. When slippage occurs, the film tilts and produces vibrations causing changes in the value of the piezoresistors. Yamada et al. [4] built a skin featuring rounded ridges equipped with strain sensors in between to detect slippage due to sensor deformation. Slippage information is extracted from the velocity and acceleration of the strain gages deformation. Tremblay et al. [5] used nibs on top of the skin surface which vibrate when an object starts to slip. Accelerometers placed inside the artificial skin capture the vibration and convey slippage notification. Schmidt et al. described in [6] a sensor made from capacitive membranes on top of which brushes of fibers were placed. Such sensors are able to detect slippage on a robot hand by fibers vibration. In [7], slippage is detected by a sudden change in the three-axial force sensor which Edin et al. developed. The technique used is to embed three metal-based strain gages at the tip of the fingers in the three axial directions. Optics is an additional option in detecting slippage, according to [8]. Using conical feelers on rubber sheet surface, Ohka et al. acquired an image of the contact area and of the feelers displacement to determine the surface normal and shear forces. Other method for detecting slippage is to consider tactile information as a tactile image and use motion detection algorithms [9]. An array of identical electrical circuits is sensitive to temporal and spatial changes, and thus identifies microvibrations produced by slip. A survey on the state of tactile sensing in robotics was done by Dahiya et al. in [10] where various such technologies are comprehensively discussed.

Prosthetics requirements are not trivial. They stem from the need of correlating machine interfacing technology with human afferent and efferent mechanisms. The demands enumerate light devices, which entail less or smaller electronics and less wires, fast communication which further assumes low algorithmic complexity, intuitive feedback modalities and intuitive feedback signals. Feedback modalities are assumed to relay meaningful information in accord with the mechanism of skin receptors. Our contribution aims at developing tactile sensing able to relay enhanced information about slippage events, while diminishing much of the electronic and algorithmic complexity often required in other tactile sensing approaches. We propose an artificial ridged skin which encodes, through its morphology, the slippage detection and slippage speed for a robotic hand. The features of the tactile signal can readily be converted to pulses patterns suitable for tactile feedback in prosthetics. The current approach emphasizes the importance of morphological properties, as a mean to outsource computational costs to mechanical structures. Pinpointing the role morphology plays, we can use it to filter meaningful information for the user and consequently to mitigate his cognitive effort in interacting with a prosthetic device. A careful design of the

This work is supported by the Swiss National Science Foundation project # k-23k1-116717/1.

Dana D. Damian, Harold Martinez, Konstantinos Dermitzakis, Alejandro Hernandez-Arieta and Rolf Pfeifer are with the Artificial Intelligence Laboratory, University of Zurich, Switzerland damian@ifi.uzh.ch

sensing interface is decisive in achieving a smoother human-robot integration.

In the following sections, we will present the tactile sensing system we developed, detailing its features, the results in creating an interface for prosthetics and close with a discussion about the contribution of this work and future directions.

II. The Artificial Skin Construction

The aim of this work is to build a tactile sensing system which takes into account the aforementioned demands in prosthetics. To accomplish this, we resorted to mechanical structures that are able to intrinsically encode information about the slippage of an object. We built a set of ridged artificial skins in which we discretely varied the distance between two consecutive ridges, D_{rr}, from 2.5 to $4mm$. The ridged artificial skin is built from silicone and transduces the surface events to a force sensing resistor (FSR) beneath. Figure 2 depicts a sample of the silicone ridged skin, the standard FSR sensor, and illustrates the process of construction. The ridged shapes of the skin were obtained by solidifying the silicone into an ABS ridged mask which was built by rapid prototyping. The transverse sectional shape of the silicone ridge is an equilateral triangle, with the side $L = 2.5mm$. The thickness of the pad on which the ridges lay is $1mm$. The FSR sensor size is 4x4cm, measuring a force sensitivity from $100g$ to $10kg$. In between the FSR sensor and the ridged patch we placed a fabric imbibed on each side with a different type of glue to match the adhesive properties of both parts that were blended. The components are not expensive, and the construction process makes the skin sample easy to replicate.

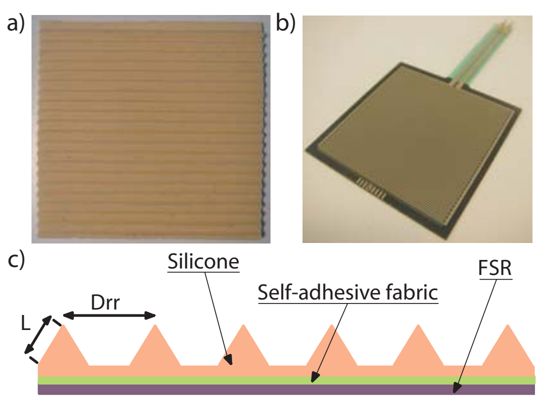

Fig. 2. The fabrication process of the ridged skin. a) Sample of ridged skin. b) Force Sensing Resistor. c) Artificial skin layers.

III. The Artificial Skin Model

The morphology of the skin in the interaction with a slipping object leaves an imprint on the FSR signal, as depicted in red in Figure 4 a). We modeled the signal acquired by the FSR sensor in two representative cases within the slippage phenomenon. In the first case, the object presses on the ridges, without deforming them laterally as in Figure 3 a). We premise that this case accounts for the valleys of the FSR signal. In the second case, the object makes contact with the first ridge in its direction of slippage, as described by Figure 3 b). The ridge deforms laterally and opposes to the object movement. Our assumption is that the FSR signal peaks are attributable to the extra-force needed to surpass the ridge in the moving direction. In Figure 3 c), a detail on the forces acting on the sliding object is illustrated. Considering the slippage velocity constant, we can extract the following relations:

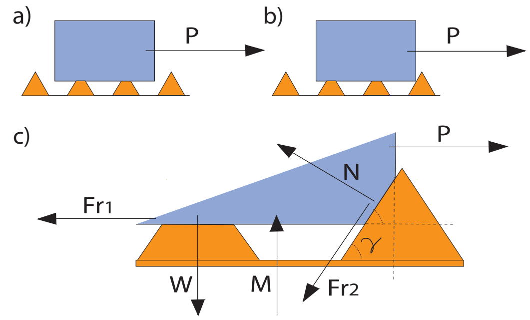

Fig. 3. Force analysis at slippage. a) Object presses on the ridges. b) Object deforms laterally the first ridge encountered in the moving direction. c) Detail on the forces in case b).

$$\begin{aligned} P - F_{r1} &= N \sin\gamma + F_{r2} \cos\gamma \\ &= N \sin\gamma + \mu N \cos\gamma. \end{aligned} \quad (1)$$

In this equations, P represents the force that pulls the object along a slipping direction. F_{r1} and F_{r2} denote friction forces, μ is the friction coefficient equal to 0.7813, and $\gamma = 60°$ is the angle of the triangular ridge. The silicone ridge opposes the movement of the object according to the value of force N. The FSR sensor underneath the ridged patch is able to detect normal forces, therefore we are interested in measuring the forces acting against this sensor. Thus the model of the FSR sensor can be formalized as in the equation bellow:

$$\begin{aligned} M(t) &= W(t) + N \cos\gamma \\ &= (1 - k\mu)W(t) + kP. \end{aligned} \quad (2)$$

The transduced value of M is modulated by the morphology of the skin. This evidence is embedded in the expression of $k = \cos\gamma/(\sin\gamma + \mu\cos\gamma)$. $W(t)$ represents the partial weight of the object gradually covering the area of the FSR during the movement. Its value depends on the ratio of the displacement between the moving object and the FSR sensor to the length of the object. Relation 2 was obtained by replacing N with its expression derived from equation 1. Eventually, the FSR model is mainly influenced by the object weight and the force transmitted by the extra-work of pulling force P. We experimentally tested the model. By measuring the FSR value when the object slips horizontally on a flat skin, we acquired the value of transduced weight in time. To explain the effect of ridges on the extra-force in the FSR signal, we measured the pulling force on the object slipping over the ridged skin. The object was pulled by a DC

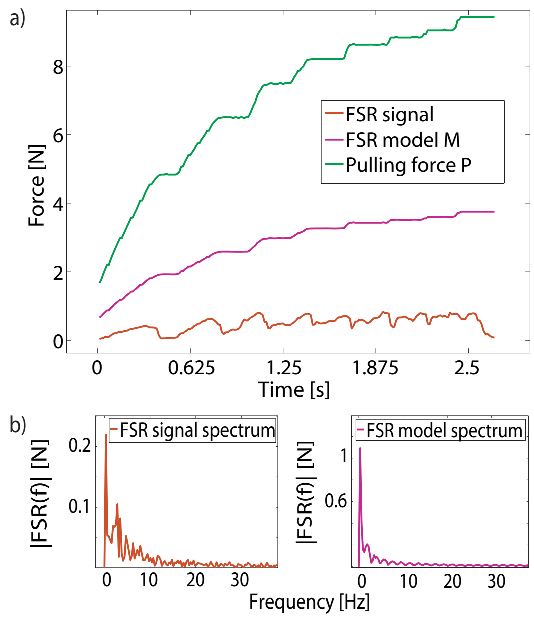

Fig. 4. FSR model. a) Time series of raw FSR (red), pulling force (green) and resulting FSR model (magenta). b) Frequency spectrum of raw FSR and model FSR showing identical peak frequencies of $0.315Hz$.

motor at constant speed. The pulling force P was measured using a potentiometric force sensor wired in series with the object. We simultaneously acquired the values of the FSR and of the potentiometric force sensor during the slippage trial. Feeding the values from the time series of the signals into the model equation, we obtain the FSR model denoted in Figure 4 a). A Fast Fourier Transformation applied to the raw FSR signal (red) and to the FSR model (magenta) discloses that the two signals have the same frequency equal to $0.315Hz$. This is illustrated in Figure4 b) by the highest peak in the signals spectrum. The inaccuracies of the model stem from various reasons: (1) the friction force becomes larger as the moving object covers more of the surface of the FSR sensor, subsequently increasing the pulling force; (2) we ignore the elastic deformation in our model, which would also absorb energy from the moving object, and (3) the mechanical tolerance of the potentiometric force sensor which has a built-in spring. The above equations also apply for skewed orientation of the plane along which the object slips.

IV. The structural properties of the ridged artificial skin

The bio-mechanical complexity of the ridges on the human hand is still an intriguing research topic. Their role is debated from sensing to dexterity [11]. The ridged structure offers better grip due to increased friction [12], it magnifies the pressure exerted by the manipulated object [13] and acts as a frequency filter for specific skin mechanoreceptors [14]. In this section, we present the characteristics of the ridged artificial skin we built, under different force conditions.

1) The artificial skin as a force transducer: For a static characterization of the force, we tested several types of artificial skins while various weights were placed on top. The artificial skins had different ridge densities designated by the inter-ridge distance (D_{rr}). A flat skin (without ridges) was also used for reference ($D_{rr} = 0.0mm$). Four trials were performed for each skin and each weight. The data acquisition was made by a Texas Instruments DAQ system, sampling at $1000Hz$, and further analyzed in Matlab. Figure 5 depicts the voltage amplitude elicited by the skin patches when weights of 100 to $1000g$ were placed on top. For each weight, the data shows a relative increased voltage value with reduced ridge density. The maximum standard deviation was $0.13V$ for the skin with $D_{rr} = 3.75mm$, followed by the skin with $D_{rr} = 3.0mm$ with standard deviation of $0.11V$. The inter-ridge distance affects force measurement in that the contact surface distributes force according to the number of ridges supporting the object, when the object is larger than the sensorized skin patch. This implies increased force values for large inter-ridge distances and decreased force values when ridge density is high. These tendencies can be seen to some extent in Figure 5 if we ignore the two skins with high variance.

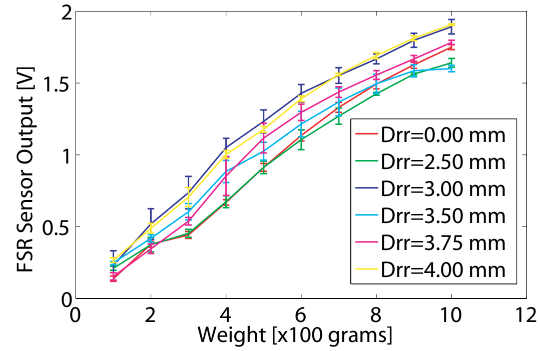

Fig. 5. Distribution in voltage magnitude as a response to different object weights and inter-ridge distances D_{rr}.

2) The artificial skin as a slippage detector: Grip disturbances can lead to the slippage of a grasped object. To stabilize the object in the hand, it is mandatory to detect such events. Additionally, slippage speed can provide preliminary cues to regulate grip force when the friction coefficient is known [2]. We conducted experiments with a sliding object to quantitatively evaluate slippage speed. We utilized six types of artificial skins and applied a total of three slippage velocities. To cover the entire surface of the artificial skin, we placed two FSR sensors beneath. The results are invariant to the number of FSRs and this grants skin efficiency even with one single FSR. However, there is no such standard sensor that has the size of the particular skin we built. In a typical experiment, an object was sliding horizontally across the artificial skin at a constant speed given by a DC motor running at preset parameters. The skins were fixed to exclude extraneous vibrations. The data acquisition was made by the system described in 1) and a peak frequency was extracted from the spectrum of the data.

The time series in Figure 6 show the signature of the slippage signal with respect to the inter-ridge distance pa-

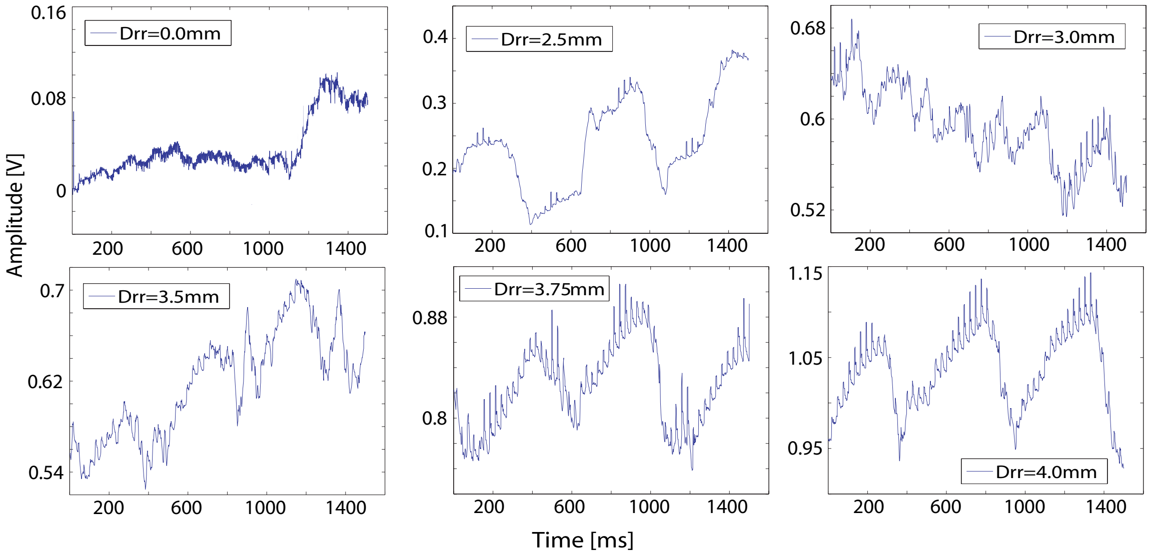

Fig. 6. Time profiles for slippage signals generated by an object sliding at same speed over skins of different inter-ridge distances D_{rr}.

rameter, at a constant slippage velocity of $10mm/s$. In the spectrum, the ridge patterns gave rise to meaningful peak frequencies, in contrast to the flat artificial skin. The latter one maintained a low amplitude in time and the yielded frequency was being assigned, for most trials, the smallest frequency in the spectrum, regardless of slippage velocity.

Our model described in section III suggested that each time the sliding object encountered a ridge, the signal recorded a peak value. Thus, under slippage conditions, the skin patch behaves like a signal generator whose frequency f_s accounts for slippage speed v_o of the object and for distance D_{rr} between two consecutive ridges. Given a constant velocity, this relation can be expressed as follows:

$$f_s = \frac{1}{\Delta t} = \frac{v_o}{D_{rr}}.$$

where Δt is the period between two consecutive peaks in the signal. By statistically averaging the measured velocity of the moving object across experimental trials, we were able to calculate the ideal frequency. The results depicted in Figure 7 show values of peak frequencies extracted for the six skins and three velocities. They suggested that inter-ridge distance D_{rr} is an important parameter for the quality of frequency encoded information. Among all skins, the one with $D_{rr} = 4.0mm$ yielded discriminatory peak frequencies for each velocity. Furthermore, its mean value was the closest to the ideal frequency given by the formula above. The peak frequency was computed as an average over five experiments per skin per velocity.

V. The Informational Properties of the Ridged Artificial Skin

In our experiments for prosthetics we utilize the robotic hand [15] depicted in Figure 1. Our goal is to achieve a fully integrated system, comprising of a user which can control a robotic hand via bio-electrical signals, and of a robotic

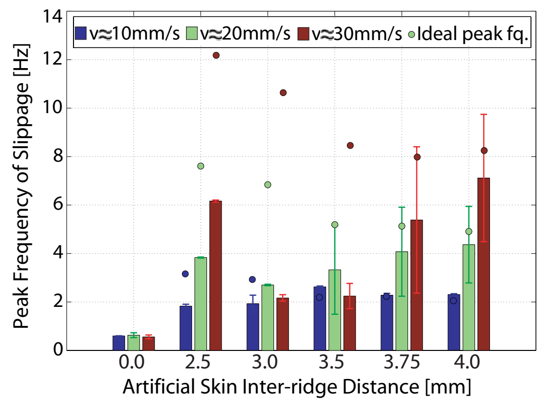

Fig. 7. Peak frequencies of slippage signal at three velocities as elicited by skins with different inter-ridge distances D_{rr}.

hand which in turn is able to efficiently acquire information about grasping events and transmit it back to the user. In this section we describe the experiment to evaluate slippage detection in the robotic hand, and the implementation of a tactile feedback encoding, to complete part of this prosthetic loop, as illustrated in Figure 8.

A. Slippage detection in robotic hand

This experiment was intended to test the robotic hand performance in slippage detection in a dynamical and noisy environment. The robotic hand is tendon driven and has 13 degrees of freedom. Its palm was equipped with a 8x4cm patch of ridged artificial skin. It was only this area of the robotic hand which was investigated for slippage detection, the fingertip skin was inactive. We conducted our experimental trials with the robot hand equipped with the ridged artificial skin of $Drr = 4.0mm$. Two FSR sensors underneath the skin recorded the surface events. The sensors values were acquired at $80Hz$. A Fast Fourier

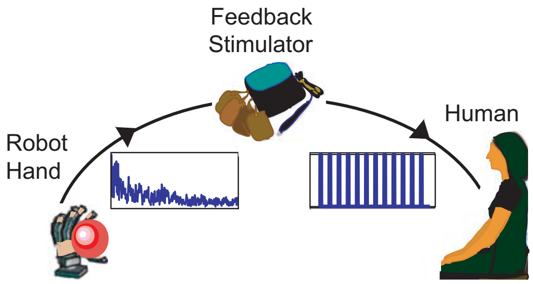

Fig. 8. Schematics of tactile sensing system. Artificial skin encodes slippage whose speed is further encoded into pulses frequency for stimulating user in prosthetic applications.

Transformation was run over the time series and a peak frequency was extracted. We used two types of objects, a rectangular and a cylindrical object. One object was slipping horizontally across the skin at a certain speed set by a DC motor. The robotic hand was programmed to automatically tighten the grip in order to hold the object in the palm. The motors of the robotic hand were actuated proportionally to the peak frequency to flex the fingers toward the object: motors flexed the fingers faster when frequency was high and flexed them slower when frequency was low. Stable grasp was discriminated as a stable signal over a period of 12.5 milliseconds, while slippage was classified mainly by a peak frequency occurring in a range spectrum of $[1, 20] Hz$. Figure 9 shows the performance of the robot hand in gripping and stopping an object from slipping away, when the object slided over its skin at six velocities. Ten trials per speed for each object were run. The success at sliding speeds lower than $10 mm/s$ maintained higher than 90%. However, at slippage speeds larger than $17 mm/s$, the performance degraded drastically. The rate of failure was higher for the cylindrical than for the rectangular object. One explanation is that the contact surface between the cylindrical object and the ridged skin is reduced compared with the rectangular object, thus decreasing the accuracy in detecting an appropriate slippage frequency. Systematic analysis to evaluate the relation between the slippage frequency and the slippage velocity was not conducted because it was not possible to control all the experimental conditions (noise from the motors, mechanical disturbances of the robotic fingers tightening around the object, etc).

B. Feedback encoding of the slippage signal

Based on the findings of our study, we propose an implementation for the feedback stimulation in prosthetics to relay information about slippage events to users. A promising prosthesis is one which combines the precision of the robotic device in mechanical events with the experience of the user capable of discerning best among contextual information. Tactile feedback provides to users notification on grasping events and decisional control over the reaction requested by such events. An automated prosthesis would deprive the user of sensorial and manipulative re-education, making the integration between the user and the prosthesis cumbersome. Thus, tactile feedback signal becomes of major importance for the prosthesis effectiveness [16]. One way to deliver the tactile feedback is vibrations. Vibration is the sensation produced by sinusoidal waves of objects that are put against the skin [17]. The response of skin mechanoreceptors is to signal an action potential to each cycle of the oscillation. This kind

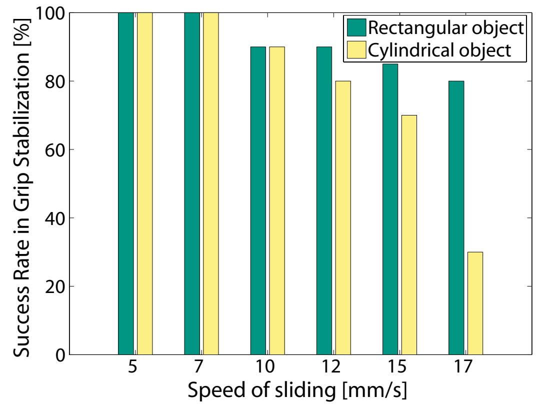

Fig. 9. Performance in robotic hand grip stabilization, as a response to object slippage at six speeds.

of mechanism is proposed to encode the slippage detection and speed to tactile stimulation feedback in prosthetics in order to alert the user to object slipping. This is possible due to the series of ridges which pulse when a slipping object makes contact with them. Therefore, slippage frequency extracted from the skin recordings can be readily converted to vibration frequency through linear mapping. In Figure 10, two instances of pulse stimulation patterns are presented (b)) for two slippage signals whose frequencies are equal to 2 and $4 Hz$ (a)). The slippage frequencies were scaled onto vibration frequencies of range $[1, 150] Hz$ to meet somatosensory physiological constraints [18]. Additionally, the pulses have constant width to maintain same level of tactile stimulation intensity. This way, the vibration frequency information can be better decoupled from its intensity component [19], and the slippage speed better discriminated.

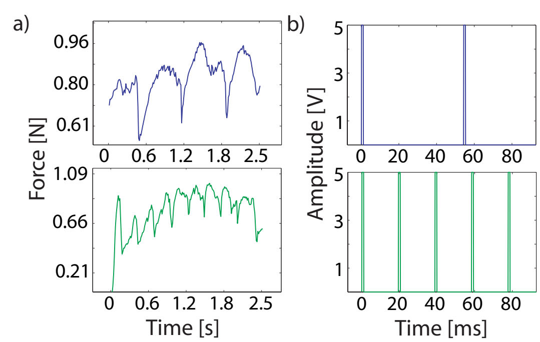

Fig. 10. Feedback stimulation patterns. a) Two slippage signals with frequencies of $2Hz$ (top) and $4Hz$ (bottom). b) Expected stimulation pulses corresponding to signals in a).

VI. DISCUSSION

1) The ridge pattern: The design of the artificial skin ridges was minimal, drastically simplifying the properties of the biological hand ridges. We ignored the elliptical or curved arrangement of the ridges, and chose a linear one with same ridge orientation. Therefore, to avoid results of cases we did not treat, our experiments were performed with objects only sliding perpendicularly across the ridges. Otherwise, the accuracy in detecting the slippage frequency would decrease drastically.

2) The inter-ridge distance: The current setup is able to correctly detect slippage for objects heavier than $70N$, which slip at speeds lower than approx. $15mm/s$. The range of inter-ridge distances we used is justified by assumptions for sensing efficacy. We premised that a D_{rr} lower than $2.5mm$ would dismiss an accurate slippage sense, within the same trend as the skin with $D_{rr} = 2.5mm$. However, we hypothesize that the skin model can be replicated at smaller scales maintaining the same behavior if concurrently, the raw sensor it is used with has greater precision. On the other hand, a skin with D_{rr} greater than $4mm$ would make the slippage sense more coarse, taking additional time to compute the FFT and deliver the result in feedback stimulation.

3) The vibro-tactile feedback: For daily activities in which users are engaged, it is important that they receive not only on-off event information (on-off contact with objects, on-off slippage detection) about grasping events, but also continuous information on dynamical haptic events (slippage of an object, grasping force changes). We transmit continuous slippage by discrete timed events, according to neuroscience findings [20] which advocate that the brain responds better to discrete movements than to continuous actions. Such discrete stimulation, in contrast to static one, also suffers less from habituation [18]. The quantification of slippage speed within the stimulation supports the user perception of a slippage notification or alarm to which he should react with an appropriate grip. Apart from signaling slippage, this specific feedback pattern could also provide the users with morphological cues about the robotic device embedded to their body. Ultimately, we hypothesize that exposing the users to such dynamical and relevant information about the interaction with the environment would reinforce the incorporation of the robotic device into the body.

VII. CONCLUSIONS AND FUTURE WORK

In this study, we showed that a careful consideration of morphology in the design of tactile sensing systems can lead to enhanced prosthetic interfaces, with reduced cost on the overall complexity of the prosthetic system. The ridges of the artificial skin allowed the encoding of slippage detection and slippage speed quantification into a signal which can be readily postprocessed for feedback stimulation patterns in prosthetics. As a follow up, an investigation of other morphologies for the artificial skin, like spiral or concentric circular ridges will take place. Our preliminary results with circular ridges reveal that we can to an extent extract information about relative position of an object in the hand. Future work will also involve tests with human participants to evaluate the effectiveness of the proposed stimulation pattern in detecting slippage and adjusting grip.

REFERENCES

[1] G. Robles-De-La-Torre, "The importance of the sense of touch in virtual and real environments," *IEEE Multimedia, Special issue on Haptic User Interfaces for Multimedia Systems*, vol. 13, no. 3, pp. 24–30, 2006.

[2] R. Johansson and G. Westling, "Roles of glabrous skin receptors and sensorimotor memory in automatic control of precision grip when lifting rougher or more slippery objects," *Exp Brain Res.*, vol. 56, no. 3, pp. 550–564, 1984.

[3] D. P. J. Cotton, A. Cranny, N. M. White, and P. H. Chappell, "A thick-film piezoelectric slip sensor for a prosthetic hand," *IEEE Sensors Journal*, vol. 7, no. 5, pp. 752–761, 2007.

[4] D. Yamada, T. Maeno, and Y. Yamada, "Artificial finger skin having ridges and distributed tactile sensors used for grasp force control," *Journal of Robotics and Mechatronics*, vol. 14, no. 2, pp. 140–146, 2002.

[5] M. Tremblay and M. Cutkosky, "Estimating friction using incipient slip sensing during a manipulation task,," in *IEEE Proc. Int.Conf .on Robotics and Automation*, vol. 1, 1993, pp. 429–434.

[6] P. Schmidt, E. Mal, and R. Wrtz, "A sensor for dynamic tactile information with applications in humanrobot interaction and object exploration," *Robotics and Autonomous Systems*, vol. 54, no. 12, pp. 1005–1014, 2006.

[7] B. Edin, L. Ascari, L. Beccai, S. Roccella, J.-J. Cabibihan, and M. Carrozza, "Bio-inspired sensorization of a biomechatronic robot hand for the grasp-and-lift task," *Brain Research Bulletin*, vol. 75, no. 6, pp. 785–795, 2008.

[8] M. Ohka, Y. Mitsuya, I. Higashioka, and H. Kabeshita, "An experimental optical three-axis tactile sensor for micro-robots," *Robotica*, vol. 23, no. 4, pp. 457–465, 2005.

[9] R. Maldonado-Lopez, F. Vidal-Verdu, G. Linan, E. Roca, and A. Rodriguez-Vazquez, "Early slip detection with a tactile sensor based on retina," *Analog Integr Circ Sig Process*, vol. 53, pp. 97–108, 2007.

[10] R. Dahiya, G. Metta, M. Valle, and G. Sandini, "Tactile sensing from humans to humanoids," *IEEE Transactions on Robotics*, vol. 26, no. 1, pp. 1–20, 2010.

[11] M. Venkadesan and F. Valero-Cuevas, "Neural control of motion-to-force transitions with the fingertip," *Journal of Neuroscience*, vol. 28, no. 6, p. 13661373, 2008.

[12] M. Cartmill, "The volar skin of primates: its frictional characteristics and their functional significance," *American Journal of Physical Anthropology*, vol. 50, pp. 497–510, 1979.

[13] R. Fearing and J. M. Hollerbach, "Basic solid mechanics for tactile sensing," *The International Journal of Robotics Research*, vol. 4, no. 3, pp. 40–54, 1985.

[14] J. Scheibert, S. Leurent, A. Prevost, and G. Debregeas, "The role of fingerprints in the coding of tactile information probed with a biomimetic sensor," *Science*, vol. 13, no. 323(5920), pp. 1503–1506, 2009.

[15] A. H. Arieta, R. Kato, H. Yokoi, and W. Yu, "Development of a multi-dof electromyography prosthetic system using the adaptive joint mechanism," *Applied Bionics and Biomechanics*, vol. 3, no. 2, pp. 101–111, 2006.

[16] A. H. Arieta, C. Dermitzakis, D. Damian, M. Lungarella, and R. Pfeifer, *Sensory-motor coupling in rehabilitation robotics*. Vienna, Austria: Handbook of Service Robotics, I-Tech Education and Publishing, 2008.

[17] E. Kandel, J. Schwartz, and T. Jessell, *Principles of Neural Science, 4th edn.* New York,USA: McGraw-Hill, 2000.

[18] K. A. Kaczmarek, J. G. Webster, P. B. y Rita, and W. J. Tompkins, "Electrotactile and vibrotactile displays for sensory substitution systems," *IEEE Transactions on Biomedical Engineering*, vol. 38, pp. 1–16, 1991.

[19] A. H. Arieta, "Development of a multi-channel functional electrical stimulation system for prosthetic applications of limbs." *Doctoral Dissertation.*, 2007.

[20] R. Spencer, T. Verstynen, M. Brett, and R. Ivry, "Cerebellar activation during discrete and not continuous timed movements: An fmri study," *NeuroImage*, vol. 36, no. 2, pp. 378–387, 2007.